



# Numerical simulation of multi-species transport through saturated concrete during a migration test — *MsDiff* code

Olivier Truc<sup>a,b,\*</sup>, Jean-Pierre Ollivier<sup>a</sup>, Lars-Olof Nilsson<sup>b</sup>

<sup>a</sup>Laboratoire Matériaux et Durabilité des Constructions, Complexe Scientifique de Rangueil, INSA Génie Civil, F-31077 Toulouse, France

<sup>b</sup>Department of Building Materials, Chalmers University of Technology, SE-41296 Gothenburg, Sweden

Received 21 December 1999; accepted 11 May 2000

## Abstract

A numerical model, called *MsDiff* (Multi-Species DIFFusion), based on a finite difference method and on the Nernst–Planck relation has been developed. The concentration profiles for several species (i.e.,  $\text{Cl}^-$ ,  $\text{Na}^+$ ,  $\text{K}^+$ , and  $\text{OH}^-$ ), the flux and the potential profile are computed. The simulations allow having a better understanding about the phenomena involved during the transport of different ions into concrete under the influence of an electrical field. The effect of various parameters as the pore solution composition, the non-ideality of the solutions or the chloride binding, is also discussed. Finally, it is shown how the effective diffusion coefficient of chlorides could be measured experimentally by using the LMDC test method. © 2000 Elsevier Science Ltd. All rights reserved.

**Keywords:** Numerical model; Chloride ions; Migration tests; LMDC test method

## 1. Introduction

The transport of chlorides into saturated concrete is a complex process [1–4]. Different parameters, which influence more or less the rate of penetration of chlorides [5], are necessary to describe the diffusion process of these ions. One parameter that is of great importance is the effective diffusion coefficient. A relevant and reliable test method is required in order to obtain this parameter with an acceptable accuracy. Various methods already exist but they are either time consuming or they have too many drawbacks [1,6,7].

A new method, called LMDC test method [6,8], has been developed recently in order to avoid all these problems. Nevertheless, the effective diffusion coefficient obtained from this method can vary with experimental conditions which is of course not satisfactory since there is only one diffusion coefficient of chlorides for a particular concrete. Indeed, this coefficient can be defined from the diffusion

coefficient of the ions in a pure solution  $D_0$  and from the geometry of the concrete (i.e., tortuosity ( $\tau$ ), porosity ( $p$ ), and constrictivity ( $\epsilon$ )) in which the transport process occurs [9] (Eq. (1)):

$$D_e = p \frac{\tau}{\epsilon} D_0. \quad (1)$$

There are several definitions that can be found in literature for  $D_e$  [10]. Some researchers include the porosity and some others do not. Some definitions take into account other parameters like, for example, a fluidity factor. The fact is that if two laboratories have to measure the effective diffusion coefficient of chlorides for the same concrete at a given age and therefore for a particular geometry, they should find the same value. However, this is far from reality.

In this paper, a new numerical approach and a new code based on Matlab<sup>®</sup>, called *MsDiff* (Multi-Species DIFFusion), are presented to explain the discrepancy between experimental results. The theory that allows to simulate the transport of several species through concrete during a migration test is first described. Then, the influence of different parameters (e.g., pore solution, chloride binding, . . .) that are often neglected in the models [1,5,11] is also discussed. Finally, a procedure that explains how to determine the

\* Corresponding author. Laboratoire Matériaux et Durabilité des Constructions, Complexe Scientifique de Rangueil, INSA Génie Civil, F-31077 Toulouse Cedex 4, France. Tel.: +33-6-8968-4622; fax: +33-5-6155-9949.

E-mail address: [truc@insa-tlse.fr](mailto:truc@insa-tlse.fr) (O. Truc).

effective diffusion coefficient from the LMDC test method is presented.

## 2. Model and basic equations

The principle of the experimental system to simulate is shown in Fig. 1. The concrete sample is assumed to be saturated before the test, and therefore, the convection phenomenon can be neglected. In a general case, the flux of the different species present in the system can be written in one-dimension by using the Nernst–Planck relation [12]:

$$J_i(x, t) = -D_{ei} \left( \frac{\partial c_i(x, t)}{\partial x} + z_i c_i(x, t) \frac{F}{RT} E(x, t) + \frac{c_i(x, t)}{\gamma_i(x, t)} \frac{\partial \gamma_i(x, t)}{\partial x} \right) \quad (2)$$

where  $J_i$ ,  $D_{ei}$ ,  $c_i$ ,  $\gamma_i$ , and  $z_i$  are the flux (mol/(m<sup>2</sup> s)), the effective diffusion coefficient (m<sup>2</sup>/s), the free concentration in the bulk solution (mol/m<sup>3</sup>), the activity coefficient, and the valence number of the ionic species  $i$ , respectively.  $F$  is the Faraday constant (9.64846 × 10<sup>4</sup> C/mol),  $R$  is the ideal gas constant (8.3143 J/(mol K)),  $T$  is the temperature (K),  $x$  is the space position (m) and  $t$  is the time dimension (s).  $E$  is the electrical field (V/m). This last variable can be divided in two terms, i.e., the diffusion potential created by the movement of the different species and the external electrical field applied to the system by using electrodes (cf. Fig. 1).

In order to simplify the mathematical treatment, the current density  $j$  (A/m<sup>2</sup>) applied to the system is taken as an input of the model instead of the external electrical field. The current density and the flux of the different ionic species are linked by the following basic relation [13,14] assuming that the solution remains electroneutral:

$$j = F \sum_i z_i J_i(x, t). \quad (3)$$

By inserting Eq. (2) in Eq. (3), the electrical field can be computed:

$$E(x, t) = -\frac{RT}{F} \frac{\sum_i z_i D_{ei} \left( \frac{\partial c_i(x, t)}{\partial x} + \frac{c_i(x, t)}{\gamma_i(x, t)} \frac{\partial \gamma_i(x, t)}{\partial x} \right)}{\sum_i z_i^2 D_{ei} c_i(x, t)} \quad (4)$$

The flux of the ionic species can be calculated by inserting Eq. (4) in Eq. (2):

$$J_i(x, t) = -D_{ei} \left( \underbrace{\frac{\partial c_i(x, t)}{\partial x}}_{\text{Diffusion}} - \underbrace{z_i c_i(x, t) \frac{\sum_i z_i D_{ei} \left( \frac{\partial c_i(x, t)}{\partial x} + \frac{c_i(x, t)}{\gamma_i(x, t)} \frac{\partial \gamma_i(x, t)}{\partial x} \right)}{\sum_i z_i^2 D_{ei} c_i(x, t)}}_{\text{Migration}} + \underbrace{\frac{c_i(x, t)}{\gamma_i(x, t)} \frac{\partial \gamma_i(x, t)}{\partial x}}_{\text{Activity}} \right) \quad (5)$$

The relation to compute the concentration profiles is given by the continuity equation [Eq. (6)]:

$$\frac{\partial C_{Ti}}{\partial t} = -\frac{\partial J_i(x, t)}{\partial x} \quad (6)$$

where  $C_{Ti}$  is the total concentration (mol/m<sup>3</sup> of concrete) of the species  $i$ . This total concentration can be written, for a representative volume of concrete, as follows [Eq. (7)]:

$$C_{Ti} = p c_i + (1 - p) \rho C_{bi} \quad (7)$$

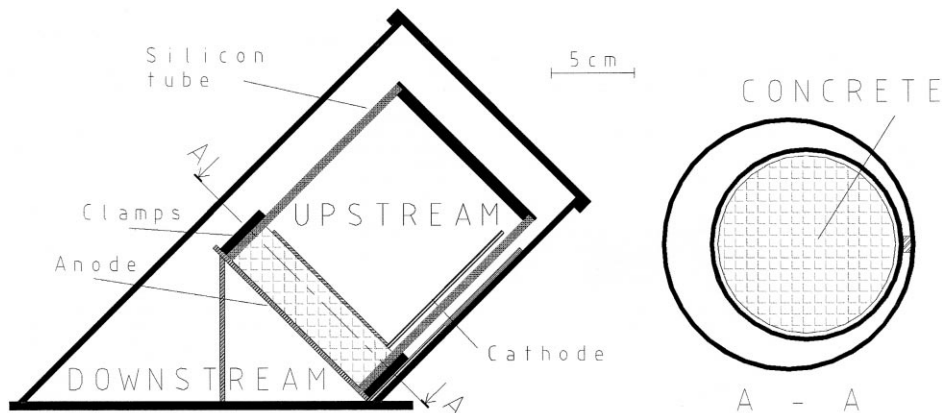


Fig. 1. LMDC diffusion test set-up.

where  $C_{bi}$  is the bound amount (mol/kg of concrete) of species  $i$  in the solid phase,  $p$  is the concrete porosity and  $\rho$  is the density of dry concrete (kg/m<sup>3</sup>).

The species considered in this paper are chloride, sodium, potassium and hydroxide. These species are the major components [15] of the pore solution and therefore it is a good approximation to limit our study to these four ionic species. In the following paragraphs,  $\text{Na}^+$ ,  $\text{K}^+$ ,  $\text{Cl}^-$ , and  $\text{OH}^-$  will be associated with the numbers  $i=1$ ,  $i=2$ ,  $i=3$ , and  $i=4$ , respectively.

It must be emphasized that chloride binding has been included in the model. The binding of chloride (physical and chemical), is described in this first approach with a Langmuir isotherm relation [Eq. (8)]:

$$C_{b3} = \frac{\alpha c_3}{1 + \beta c_3}. \quad (8)$$

This last equation [Eq. (8)] is based on the following assumptions.

- The local thermodynamic equilibrium is maintained during the migration test (instantaneous reactions). The validity of this assumption has been recently challenged by Castellote et al. [16]. Future improvements of the model should make it possible to include the rate of binding in order to verify the influence of this phenomenon on the migration test results.
- The influence of the hydroxyl ion concentration on the binding phenomena is neglected.

It is also assumed that for each chloride bound, one hydroxide is released from the solid phase so as to keep the electroneutrality of the pore solution [17]. The binding of cations has been neglected in this study and therefore their total concentration is equal to the free concentration in the pore solution.

The four species considered hereby must verify a last relation that is the local electroneutrality condition written for a representative volume of concrete:

$$\sum_i z_i c_i = 0. \quad (9)$$

Indeed, for a macroscopic system (much bigger than the Debye length), Poisson equation can be written in its dimensionless form [see Eq. (10)] [18]:

$$d\Delta\varphi = -4\pi F \sum_i z_i c_i. \quad (10)$$

This equation, which has been used recently by Samson and Marchand [11] to describe the transport of ionic species in electrolytic solutions, can be replaced by the local electroneutrality condition [13,14,18] because Eq. (10) has on the left hand side a very small parameter  $d$  (the squared ratio of the Debye length to the size of our system, i.e., few centimeters!), whereas on the other side of the same

equation there is the local charge balance. This usually implies that the system may be regarded as split into the locally electroneutral bulk solution (the one that we are studying) and the electric double layers where most of the space charge is concentrated. Indeed, according to Eq. (10) even slight deviations of its right hand side from zero, on a macroscopic scale, would require immense non-equilibrium electric fields in the system, incompatible with the moderate voltages usually used during migration tests.

On the basis of this analysis, the set of continuity equations to compute in order to obtain the free concentration profile for each species is as follows (the variables  $x$  and  $t$  are omitted for simplicity reasons,  $c(x,t)=c$ ):

$$\frac{\partial c_1}{\partial t} = -\frac{1}{p} \frac{\partial J_1}{\partial x} \quad (11)$$

$$\frac{\partial c_2}{\partial t} = -\frac{1}{p} \frac{\partial J_2}{\partial x} \quad (12)$$

$$\frac{\partial c_3}{\partial t} = -\frac{1}{p + (1-p)\rho \frac{\partial C_{b3}}{\partial c_3}} \frac{\partial J_3}{\partial x} \quad (13)$$

$$c_4 = c_1 + c_2 - c_3. \quad (14)$$

This last relation [Eq. (14)] is obtained from the electro-neutrality condition [see Eq. (9)]. By inserting this relation into Eq. (4), the electrical field can be expressed by:

$$E(x, t) = -\frac{RT}{F} \times \frac{\frac{j}{F} + L \frac{\partial c_1}{\partial x} + M \frac{\partial c_2}{\partial x} - N \frac{\partial c_3}{\partial x} + c_1 \Gamma_1 + c_2 \Gamma_2 - c_3 \Gamma_3}{d} \quad (15)$$

with (Eqs. (16) and (17)):

$$L = D_{e1} - D_{e4}$$

$$M = D_{e2} - D_{e4}$$

$$N = D_{e3} - D_{e4}$$

$$O = D_{e1} - D_{e4}$$

$$P = D_{e2} - D_{e4}$$

$$d = Oc_1 + Pc_2 + Nc_3 \quad (16)$$

$$\Gamma_1 = \left( \frac{D_{e1}}{\gamma_1(x, t)} \frac{\partial \gamma_1(x, t)}{\partial x} - \frac{D_{e4}}{\gamma_4(x, t)} \frac{\partial \gamma_4(x, t)}{\partial x} \right)$$

$$\Gamma_2 = \left( \frac{D_{e2}}{\gamma_2(x, t)} \frac{\partial \gamma_2(x, t)}{\partial x} - \frac{D_{e4}}{\gamma_4(x, t)} \frac{\partial \gamma_4(x, t)}{\partial x} \right)$$

$$\Gamma_3 = \left( \frac{D_{e3}}{\gamma_3(x, t)} \frac{\partial \gamma_3(x, t)}{\partial x} - \frac{D_{e4}}{\gamma_4(x, t)} \frac{\partial \gamma_4(x, t)}{\partial x} \right). \quad (17)$$

It will be shown later in this paper that the terms  $\Gamma_1$ ,  $\Gamma_2$ , and  $\Gamma_3$ , which include the non-ideality effect of the solu-

tion, are negligible and the last part of the theory is developed without considering them.

According to these last assumptions and by inserting Eq. (15) into Eqs. (11)–(13), the following system of dimensionless equations [Eqs. (18)–(20)] can be obtained:

$$\begin{bmatrix} p & 0 & 0 \\ 0 & p & 0 \\ 0 & 0 & p + (1-p)\rho \frac{\partial c_{h3}}{\partial c_3^*} \end{bmatrix} \cdot \begin{bmatrix} \frac{\partial c_1^*}{\partial r^*} \\ \frac{\partial c_2}{\partial r^*} \\ \frac{\partial c_3^*}{\partial r^*} \end{bmatrix} = -\frac{\partial}{\partial x^*} \left\{ \text{MATRIX} \cdot \begin{bmatrix} \frac{\partial c_1^*}{\partial x^*} \\ \frac{\partial c_2}{\partial x^*} \\ \frac{\partial c_3^*}{\partial x^*} \end{bmatrix} + \begin{bmatrix} \frac{D_{e1}^* c_1^* j^*}{d^*} \\ \frac{D_{e2}^* c_2^* j^*}{d^*} \\ -\frac{D_{e3}^* c_3^* j^*}{d^*} \end{bmatrix} \right\} \quad (18)$$

$$\text{MATRIX} = \begin{bmatrix} \left(-1 + \frac{c_1^* L^*}{d^*}\right) D_{e1}^* & \frac{c_1^* M^*}{d^*} D_{e1}^* \\ \frac{c_2^* L^*}{d^*} D_{e2}^* & \left(-1 + \frac{c_2^* M^*}{d^*}\right) D_{e2}^* \\ -\frac{c_3^* L^*}{d^*} D_{e3}^* & -\frac{c_3^* M^*}{d^*} D_{e3}^* \\ -\frac{c_1^* N^*}{d^*} D_{e1}^* \\ -\frac{c_2^* N^*}{d^*} D_{e2}^* \\ \left(-1 + \frac{c_3^* N^*}{d^*}\right) D_{e3}^* \end{bmatrix} \quad (19)$$

with

$$x^* = \frac{x}{L_0}, \quad t^* = \frac{D_0}{L_0^2} t, \quad c^* = \frac{c}{c_0}, \quad D_e^* = \frac{D_e}{D_0} \quad \text{and} \quad j^* = \frac{j L_0}{F c_0 D_0}. \quad (20)$$

The mark \* means that the variable is in its dimensionless form.  $D_0$ ,  $L_0$ , and  $c_0$  are constants that are chosen in order to have a good stability of the numerical computations. In general,  $D_0$  is the largest diffusion coefficient,  $L_0$  is the characteristic length of the system (thickness of the concrete sample), and  $c_0$  is the largest concentration. A finite difference method with an explicit scheme [19] has been used to compute the concentration profiles, the flux of the different species and the potential distribution through the concrete sample. In order to obtain results with a good accuracy, the computations were performed with 301 nodes and with a constant time step equals to 50 s.

The code, called *MsDiff*, has been developed with Matlab<sup>®</sup> 5.3(R11) and a stand-alone application was generated with the Matlab<sup>®</sup> compiler, the Matlab<sup>®</sup> Graphics Library, and C/C++ Math Library. Therefore, this program can be run on every PC without Matlab<sup>®</sup> installed on it.

### 3. Results of the simulations

#### 3.1. Influence of experimental conditions

##### 3.1.1. Influence of the chloride concentration in the upstream compartment

Several authors have noticed that the measured effective diffusion coefficient is a function of the chloride concentration [2–4,20,21]. During a pure diffusion test, it has been shown recently [22] that this variation is obtained because Fick's law is not suitable to calculate the real or intrinsic effective diffusion coefficient. Concerning the migration test, it is not quite clear if the variation observed is a true physical phenomenon, or if it is, as in the diffusion case, a bad interpretation of the experimental data.

In order to answer this question, several migration tests were simulated by using *MsDiff*. It must be underlined that these simulations were performed by using a constant current density and not a constant voltage. All the experimental conditions were kept constant except for the upstream chloride concentration. The input data used for the numerical simulations are given in Table 1. The boundary conditions were kept constant, as the duration of the test was short enough to neglect the variation of concentration in both upstream and downstream compartments.

The results for various level of chloride concentration are given in Figs. 2–5. It can be seen that even in steady state, the level of concentration for the different ions is not constant. It must also be emphasized that even in this case the flux upstream and downstream are almost the same when the steady state is reached downstream (error < 2%). That confirms previous studies performed by the authors [6,8].

From the flux of chloride calculated with the model, it is then possible to determine  $D_{eCl,exp}$  as it would be done experimentally. The expression for  $D_{eCl,exp}$  is given by the following relation, proposed by Andrade [23], which is actually a simplified version of Eq. (5):

$$D_{eCl,exp} = \frac{J_3}{c_3} \frac{RT}{FE}. \quad (21)$$

If  $J_3$  and  $c_3$  are measured by using the LMDC test method [6,8],  $J_3$  is the upstream flux and  $c_3$  is the average concentration upstream during the migration test. By doing so, it is possible to obtain the variation of  $D_{eCl,exp}$  with the chloride concentration upstream for the different simulations. The evolution determined is shown in Fig. 6. The same kind of variation has been found experimentally by doing steady state migration tests for various level of chloride concentration upstream [2,3]. Nevertheless,  $D_{e3}$  included in the model was the same for all the simulations. In fact, it can be noticed in Figs. 2–5 that

Table 1  
Input data used for the numerical simulations

(a)								
Figure number	Figs. 2–5, 7, 12, and 13			Fig. 8		Figs. 10 and 11		
$p$				0.11				
$\rho$ (kg/m <sup>3</sup> )				2300				
$j$ (A/m <sup>2</sup> )	5					0		
$D_{e1}$ (10 <sup>−12</sup> m <sup>2</sup> /s)				1.5				
$D_{e2}$ (10 <sup>−12</sup> m <sup>2</sup> /s)				2				
$D_{e3}$ (10 <sup>−12</sup> m <sup>2</sup> /s)				3				
$D_{e4}$ (10 <sup>−12</sup> m <sup>2</sup> /s)				7				
$\alpha$	$1 \times 10^{-3}$			$0 \text{ or } 1 \times 10^{-3}$		$1 \times 10^{-3}$		
$\beta$				0.3				
(b)								
Figure number	Fig. 2	Figs. 3–5	Fig. 7		Fig. 8	Figs. 10 and 11	Fig. 12	Fig. 13
			Pore solution 1	Pore solution 2				
Duration of the test (days)	0.2 or 1		1		0.1 or 1	5 or steady state	1	0.5
Length (cm)			3			1		3
Upstream concentration								
1	625	25+c <sub>3</sub> upstream			595			210
2				80				400
3	600	cf. Figs. 3–5			570			10
4				105				600
Pore solution concentration								
1		150		250	150	200		cf. Fig. 13
2		400		200		400		
3				0				
4		550		450	550	600		
Downstream concentration								
1		150		250	150	200		
2		400		200		400		
3				0				
4		550		450	550	600		

concentration gradients exist at the interfaces<sup>1</sup> between the concrete sample and the compartments even when the steady state is reached. In this case, the Eq. (21) is no longer valid because it does not take into account the diffusion term. Eq. (5) should be used instead. It means that, depending on the chloride concentration upstream and on the pore solution composition, the concentration gradients will be more or less important. Therefore, variable errors are made on  $D_{e3}$ . For some concentrations, this coefficient is underestimated and for some other concentrations it is overestimated.

These concentration gradients are developed because the conductivity of the pore solution is not the same from upstream to downstream. Indeed, it can be seen Fig. 2 that the electrical field is larger upstream than downstream because the conductivity of the pore solution is lower upstream. The conductivity is lower because chlorides

penetrate the concrete sample by replacing hydroxides. As the chloride diffusion coefficient is smaller than the one for hydroxides, the conductivity decreases.

### 3.1.2. Influence of the pore solution composition

Another parameter that influences strongly the results is the initial pore solution composition. Indeed, as in the previous case, different levels of concentration inside the sample give different concentration gradients at the interfaces in steady state. The effect of two different pore solutions composition on the measured  $D_{eCl,exp}$  from Eq. (21) have been simulated. The chloride concentration profiles simulated in both systems are presented in Fig. 7. The inputs for the simulations are reported Table 1.

In the first case, it is found that  $D_{eCl,exp} = 1.99 \times 10^{-12}$  m<sup>2</sup>/s and in the second situation  $D_{eCl,exp} = 1.68 \times 10^{-12}$  m<sup>2</sup>/s. The difference between both results is not very large because the pore solutions are quite similar. As a matter of fact, depending on the curing conditions and the mixture characteristics, the alkali content of the pore solution can be much higher (or lower) than the values considered. But, once again, it must be emphasized that

<sup>1</sup> In the present paper, the term interfaces will always refer to the surface between the ends of the concrete sample and the upstream or downstream solution.

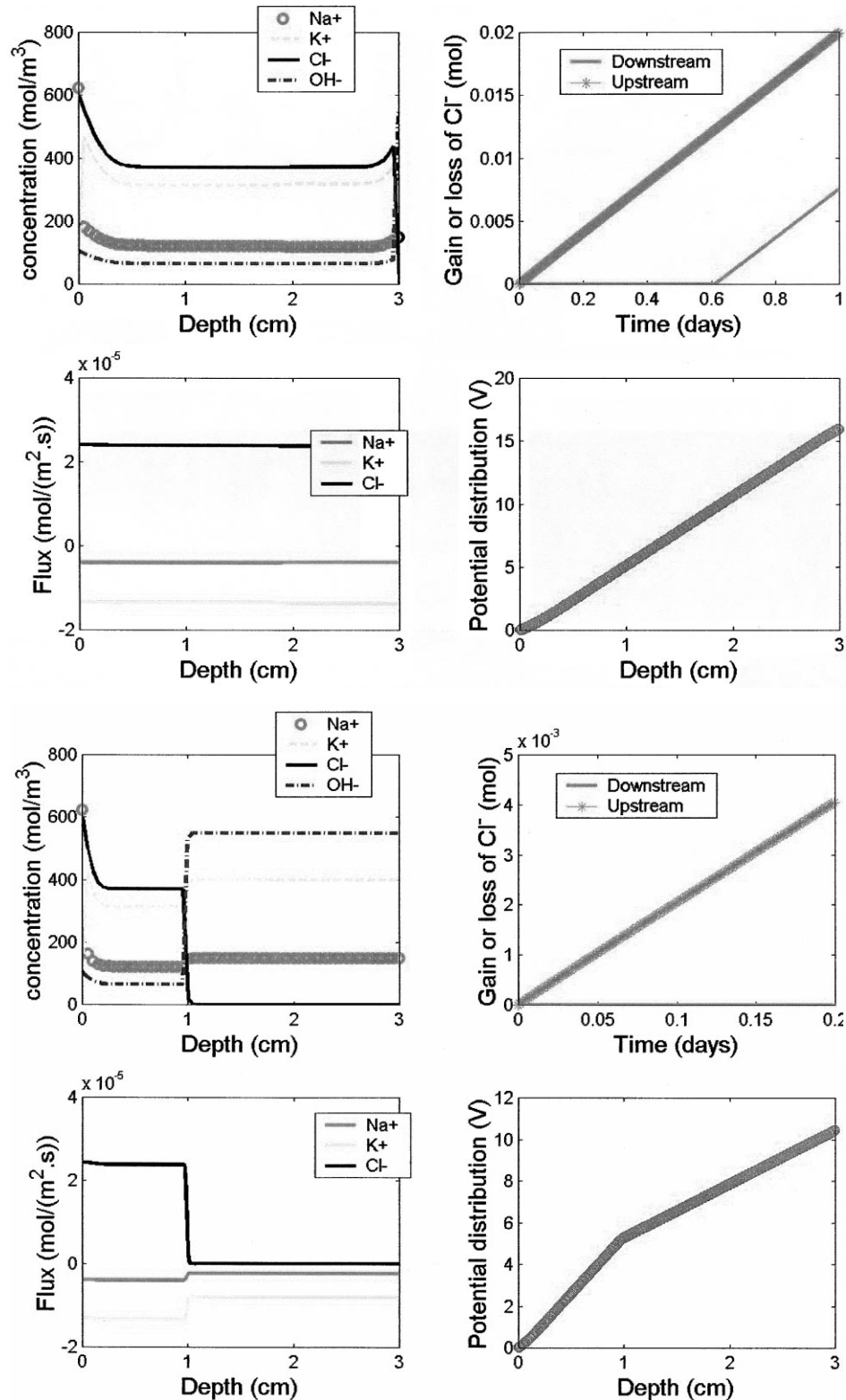


Fig. 2. Example of output datasheet obtained with *MsDiff* code (cf. Table 1 for input data). (a). Duration of the test: 1 day. (b). Duration of the test: 0.2 day.

$D_{e3}$  included in the model was still equal to the value given in Table 1. It is explained further in this paper how to limit these uncertainties on  $D_{e3}$  by using the correct experimental procedure.

### 3.2. Influence of chloride binding on the solid phase

A few experimental data can be found in literature about the rate of chloride binding during a migration

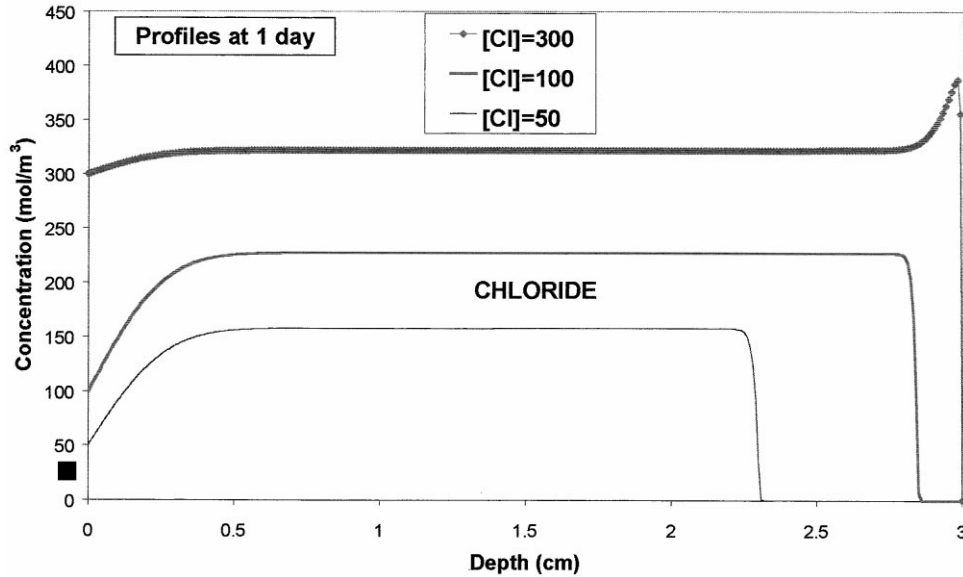


Fig. 3. Chloride concentration profiles for various  $[Cl]$  ( $\text{mol/m}^3$ ) upstream (cf. Table 1 for input data).

test [3]. The influence of the electrical field is not well established so far and the simulations are a powerful tool to understand how chloride binding can affect the results.

The free chloride concentration profiles in transient and steady states with or without considering chloride binding are shown in Fig. 8. The parameters used for the Langmuir isotherm are given in Table 1.

It appears that the binding has just a retarding effect on the process. It means that the steady state is longer to establish, but after a few hours, the differences on the level of concentration and on the concentration gradient at the interfaces are negligible.

### 3.3. Influence of the non-ideality of the solution

Recently, some investigators [11,24] discussed the effect of the non-ideality of the solutions used to perform the migration tests. By using PHRQPITZ [25] which is based on Pitzer's equations [26], the variation of the activity coefficient  $\gamma$  with the ionic strength of the electrolyte considered has been established for the different ionic species of interest in our purpose. The data obtained are given in Fig. 9.

In order to see the influence of the activity coefficient on the transport process, two systems are studied and described in Fig. 10. In these examples, the current

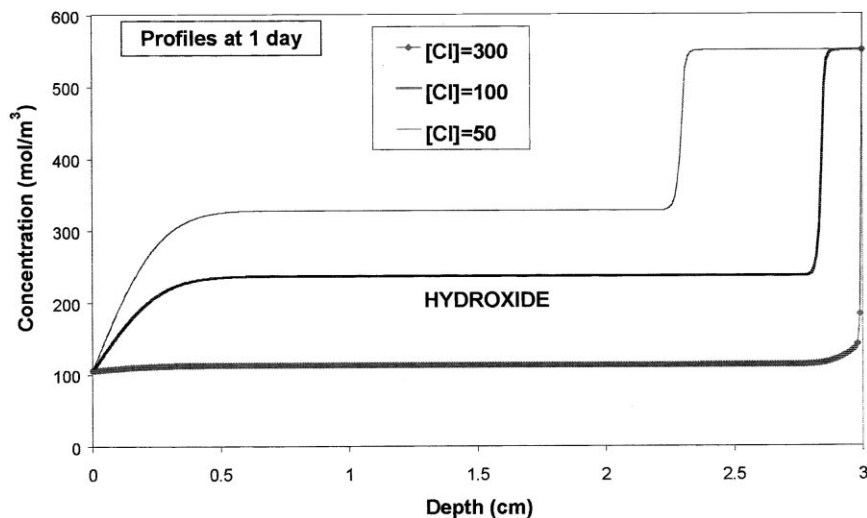


Fig. 4. Hydroxide concentration profiles for various  $[Cl]$  ( $\text{mol/m}^3$ ) upstream (cf. Table 1 for input data).

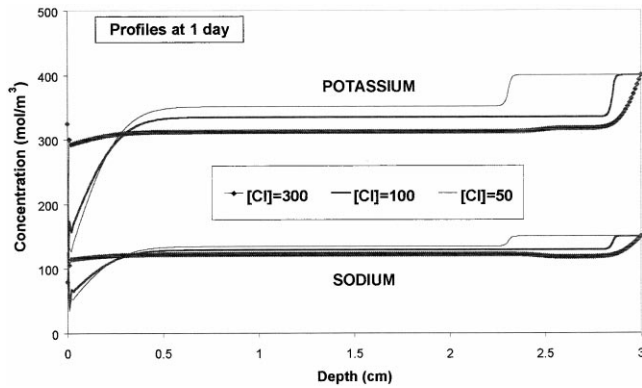


Fig. 5. Cations concentration profiles for various  $[Cl]$  ( $\text{mol/m}^3$ ) upstream (cf. Table 1 for input data).

density is assumed to be equal to 0. Therefore, a pure diffusion process is considered. Indeed, it is in this case (without external electrical field) that the non-ideality of the solution will have the stronger effect on the results according to Eq. (5).

From the data obtained with PHRQPITZ and Eq. (17) it is possible to calculate  $\Gamma_1$ ,  $\Gamma_2$ , and  $\Gamma_3$  for both systems by using a finite difference procedure. Then, the values obtained are inserted into Eqs. (4) and (5) in order to obtain the functions  $J$  and  $E$  of  $x$ . The results are presented in Fig. 11 and Table 2.

Even if the potential distributions differ only a few percents, it is obvious that the influence of the non-ideality on the fluxes and therefore on the concentration profiles is negligible as it was assumed previously in this paper. This assumption is also supported by Tang [24].

#### 4. Experimental procedure to determine the effective diffusion coefficient with the LMDC test method

The first part of this paper demonstrates that the experimental procedures that exist to measure  $D_{e3}$  are not suitable. Usually, this coefficient is calculated from Eq. (21). But, it has been shown that this equation is no longer valid when concentration gradients are present at the interfaces. Therefore, the new procedure must avoid these gradients as much as possible. Fig. 12 shows that it is possible if the chloride concentration upstream is very low (i.e.,  $0.01 \text{ mol/l}$ ) and if the concentrations for the other ionic species are the same upstream, downstream and in the pore solution. Indeed, in this case,  $D_{eCl,exp}$  measured from Eq. (21) and  $D_{e3}$  included in the model are equal (error < 3%). This is because all the concentration gradients in Eq. (5) become very small at the upstream interface in such a situation (cf. Fig. 12).

The major problem is that, a priori, the pore solution composition is unknown. Three options can be chosen at this point. The first one is to use the pore expression technique [27]. The second method is to use models that give the pore solution composition from the cement type, the ratio of water to cement, etc... [28]. Eventually, it is also possible to use a reference solution with the following composition:  $[NaOH]=200 \text{ mol/m}^3$ ,  $[KOH]=400 \text{ mol/m}^3$  upstream and downstream.  $[NaCl]=10 \text{ mol/m}^3$  is added upstream. Of course, depending on the tested concrete, the magnitude of the concentration gradients developed at the interfaces will be more or less important because of the initial pore solution composition.

Nevertheless, a sensitivity study for different pore solution compositions is shown in Fig. 13. It can be noticed that the maximum error made on  $D_{e3}$  is about 10% that is the usual discrepancy between two samples of the same concrete.

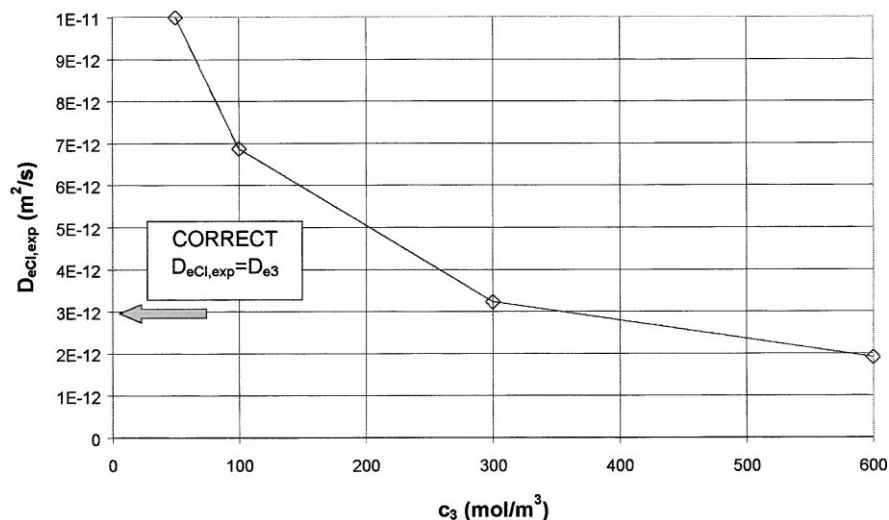


Fig. 6. Variation of the measured  $D_{eCl,exp}$  (from the model) with the upstream chloride concentration.

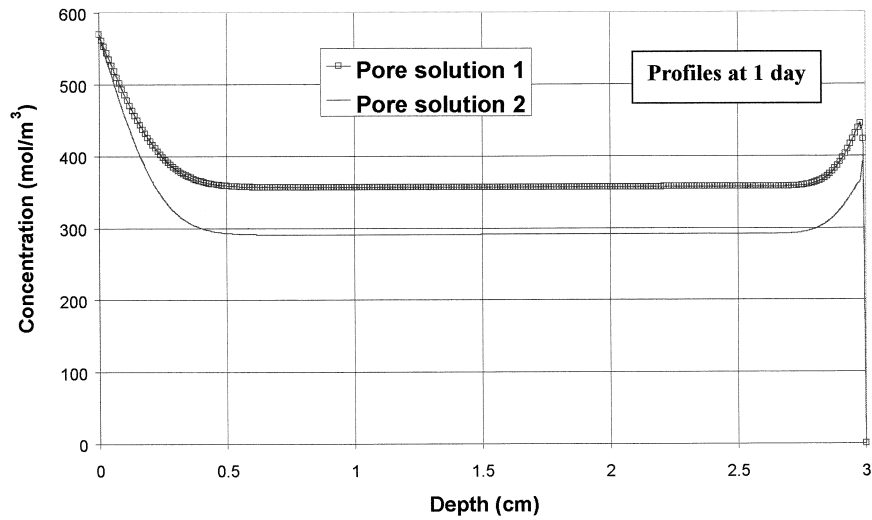


Fig. 7. Influence of the pore solution composition on the chloride concentration profiles (cf. Table 1 for input data).

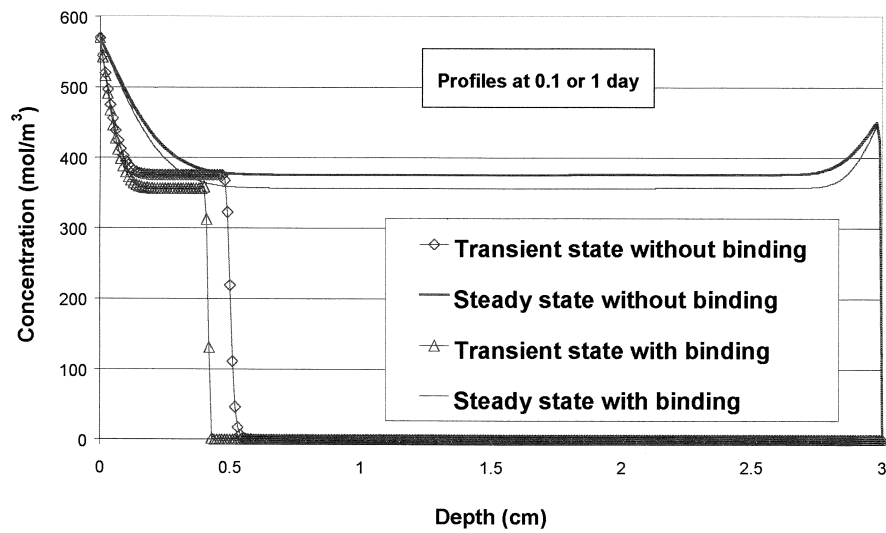


Fig. 8. Influence of the chloride binding on the transport process (cf. Table 1 for input data).

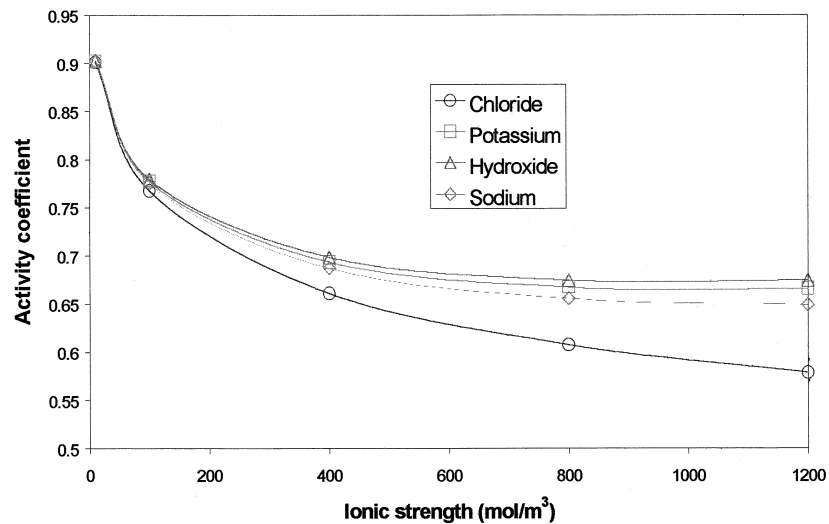


Fig. 9. Variation of the activity coefficient value with the ionic strength of the solution.

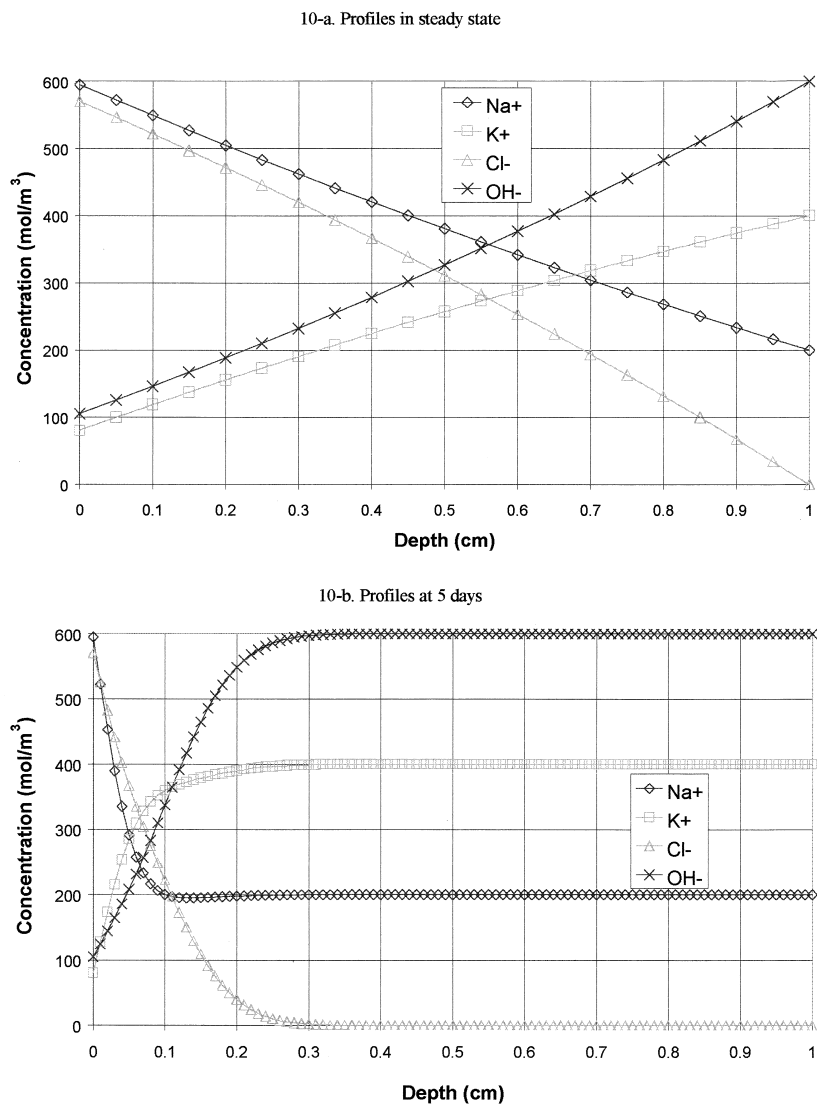


Fig. 10. Concentration profiles in steady (a) and transient (b) states to study the influence of the activity of the solutions (cf. Table 1 for input data).

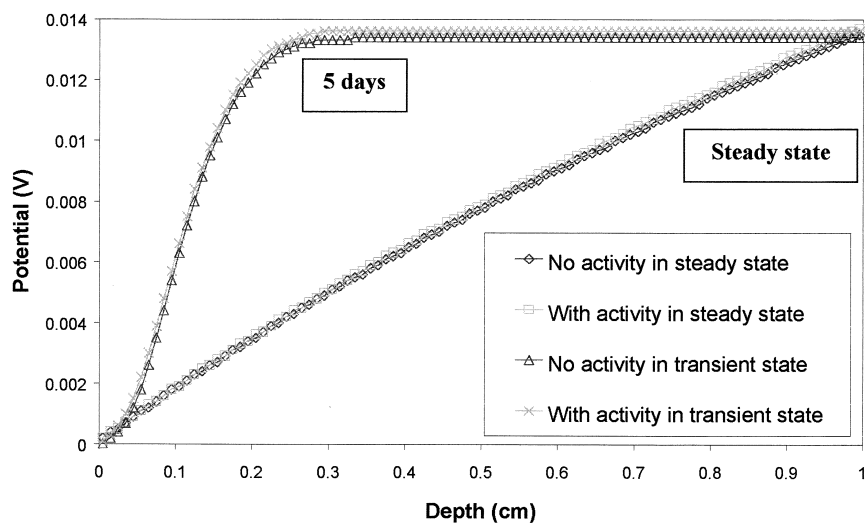


Fig. 11. Influence of the non-ideality of the electrolyte on the potential distribution (cf. Table 1 for input data).

Table 2

Influence of the non-ideality of the solution on the flux values (for  $x=1$  mm)

	No activity in steady state	Activity in steady state	No activity in non-steady state	Activity in non-steady state
Flux $\text{Na}^+$ ( $\text{mol}/(\text{m}^2 \text{ s})$ )	$7.90\text{E}-11$	$7.80\text{E}-11$	$1.22\text{E}-10$	$1.23\text{E}-10$
Flux $\text{K}^+$ ( $\text{mol}/(\text{m}^2 \text{ s})$ )	$-1.28\text{E}-10$	$-1.28\text{E}-10$	$-2.93\text{E}-10$	$-2.91\text{E}-10$
Flux $\text{Cl}^-$ ( $\text{mol}/(\text{m}^2 \text{ s})$ )	$1.14\text{E}-09$	$1.13\text{E}-09$	$5.24\text{E}-09$	$5.25\text{E}-09$
Flux $\text{OH}^-$ ( $\text{mol}/(\text{m}^2 \text{ s})$ )	$-2.47\text{E}-09$	$-2.48\text{E}-09$	$-1.37\text{E}-08$	$-1.37\text{E}-08$

Based on these interesting results, the following procedure can be applied in order to get  $D_{\text{e}3}$  with a satisfactory accuracy:

#### Materials, equipment:

Vacuum saturation equipment.  
LMDC diffusion test set-up [8].  
Chemical analysis equipment.

#### Specimens and preconditionning:

Specimens with the following dimensions can be tested:  
diameter — 10 or 11 cm,  
thickness — 1 to 5 cm.

Prior to testing, the specimens have to be saturated with alkaline solution ( $[\text{NaOH}]=25 \text{ mol}/\text{m}^3$  and  $[\text{KOH}]=80 \text{ mol}/\text{m}^3$ ) until constant weight is reached.

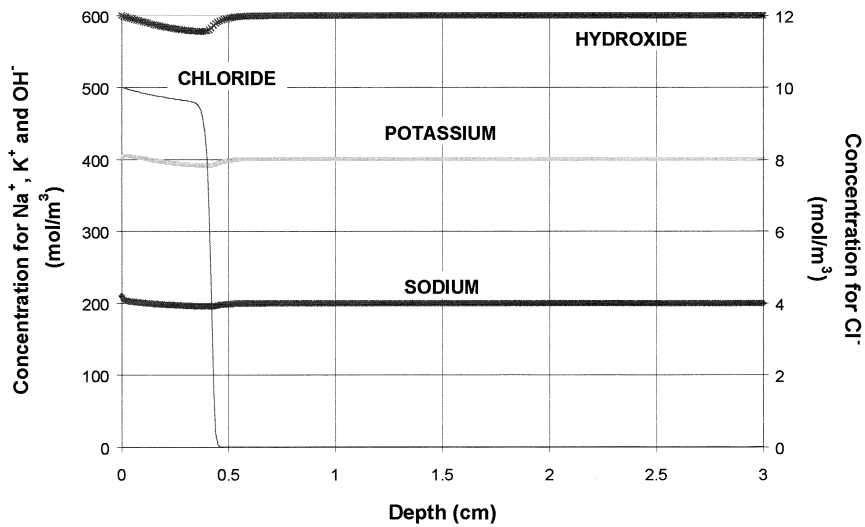


Fig. 12. Concentration profiles obtained when  $[\text{Cl}]$  is very small and the initial concentrations for the other species are the same everywhere (cf. Table 1 for input data).

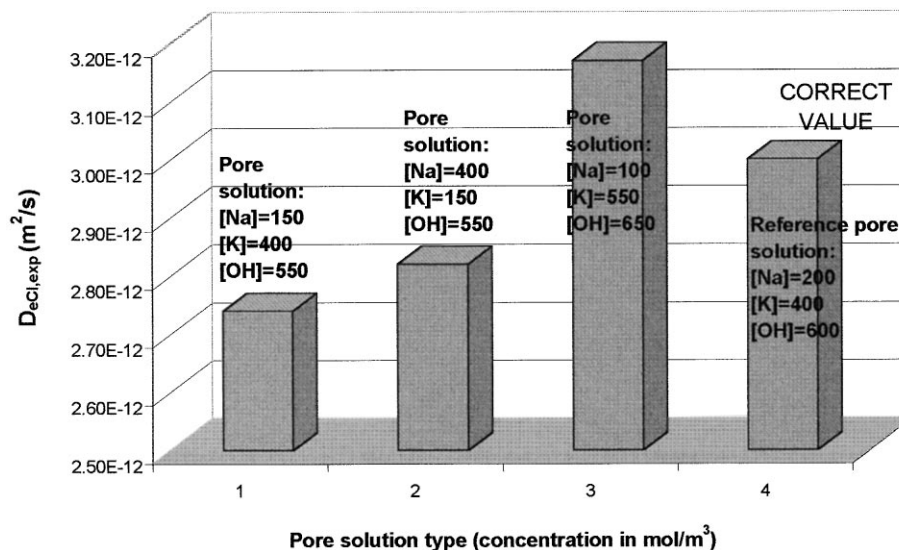


Fig. 13. Sensitivity study (cf. Table 1 for input data).

*Solutions (upstream (volume=0.5 l) and downstream (volume=2 l)):*

[NaOH]=200 mol/m<sup>3</sup>.

[KOH]=400 mol/m<sup>3</sup>.

[NaCl]=10 mol/m<sup>3</sup> is added upstream.

*Measurements:*

The chloride concentration is measured at the beginning and at the end of the test according to Truc et al. [6] in order to obtain the upstream flux  $J_3$  and the average concentration during the test  $c_3$ .

For concrete with W/C>0.5 the last of the test is about 3 days or less.

For concrete with W/C<0.5 the last of the test is about 1 week.

The sampling of the solutions for analysis has to be done with a micropipette.

*Calculation of  $D_{e3}$ :*

The effective diffusion coefficient is calculated by using Eq. (21) because by using this experimental procedure  $D_{eCl,exp} \sim D_{e3}$ .

## 5. Conclusion

From the results obtained with *MsDiff* code, it is possible to give the following conclusions concerning the transport of multi-species during a migration test.

- Because of the solutions usually used to perform the test, concentration gradients are developed at the interfaces between the concrete sample and the compartments. In this case, the simplified version of Nernst–Planck's relation (see Eq. (21)) is not valid.
- The influence of the pore solution composition is important whereas chloride binding or the non-ideality of the solutions have negligible effects on the concentration profiles in steady state.
- A new procedure is presented that allows to determine the effective diffusion coefficient of chlorides with good accuracy.

## References

- [1] L. Tang, Chloride transport in concrete — measurement and prediction, PhD thesis, Building Materials, Chalmers, Gothenburg, 1996.
- [2] T. Zhang, Chloride diffusivity in concrete and its measurement from steady state migration testing, PhD thesis, Building Materials, NTNU, Trondheim, 1997, p. 215.
- [3] J. Arsenault, Etude des mécanismes de transport des ions chlore dans le béton en vue de la mise au point d'un essai de migration, PhD thesis, Génie civil, INSA, Faculté des Sciences et de génie, Toulouse, Laval, 1999 (in French).
- [4] J.P. Bigas, La diffusion des ions chlore dans les mortiers, PhD thesis, Génie civil, INSA, Toulouse, 1994 (in French).
- [5] A. Boddy, E. Bentz, M.D.A. Thomas, R.D. Hooton, An overview and sensitivity study of a multimechanistic chloride transport model, *Cem Concr Res* 29 (1999) 827–837.
- [6] O. Truc, J.P. Ollivier, M. Carcassès, A new way for determining the chloride diffusion coefficient in concrete from steady state migration test, *Cem Concr Res* 30 (1999) 217–226.
- [7] O. Truc, J.P. Ollivier, L.O. Nilsson, Simulation de l'essai de migration, 2ème congrès universitaire de Génie Civil: "Des matériaux à l'ouvrage" AUGC, AFGC, Poitiers, France, 1999.
- [8] O. Truc, J.P. Ollivier, L.O. Nilsson, LMDC diffusion test, XVII Symposium of Nordic Concrete Research, Norsk Betongforening, Oslo, Reykjavik, Iceland, 1999, 337–339.
- [9] J.V. Brakel, P.M. Heertjes, Analysis of diffusion in macroporous media in terms of a porosity, a tortuosity, and a constrictivity factor, *Int J Heat Mass Transfer* 17 (1974) 1093–1103.
- [10] C.D. Shackelford, D.E. Daniel, Diffusion in saturated soil: I. Background, *J Geotech Eng* 117 (1991) 467–484.
- [11] E. Samson, J. Marchand, Numerical solution of the extended Nernst–Planck model, *J Colloid Interface Sci* 215 (1999) 1–8.
- [12] F. Helfferich, Ion Exchange, McGraw-Hill, New York, 1962.
- [13] S.W. Yu, C.L. Page, Computer simulation of ionic migration during electrochemical chloride extraction from hardened concrete, *Br Corros J* 31 (1996) 73–75.
- [14] A. Turnbull, Mathematical modelling of localised corrosion, in: K.R. Trethewey, P.R. Roberge (Eds.), NATO Advanced Research Workshop on Modelling Aqueous Corrosion — From Individual Pits to System Management, Kluwer Academic Publishing, Plymouth, 1993, pp. 29–63.
- [15] S. Diamond, Effects of two Danish fly ashes on alkali contents of pore solutions of cement–fly ash pastes, *Cem Concr Res* 11 (1981) 383–394.
- [16] M. Castellote, C. Andrade, C. Alonso, Chloride-binding isotherms in concrete submitted to non-steady-state migration experiments, *Cem Concr Res* 29 (1999) 1799–1806.
- [17] M. Masi, D. Colella, G. Radaelli, L. Bertolini, Simulation of chloride penetration in cement-based materials, *Cem Concr Res* 27 (1997) 1591–1601.
- [18] I. Rubinstein, Electro-diffusion of ions, *SIAM Stud Appl Math* vol. II, Philadelphia, 1990 105–111.
- [19] W.F. Ames, Numerical Methods for Partial Differential Equations, Academic Press, New York, 1977.
- [20] O. Francy, Modélisation de la pénétration des ions chlorures dans les mortiers partiellement saturés en eau, PhD thesis, Génie civil, Paul Sabatier, Toulouse, 1998 (in French).
- [21] S. Chatterji, Transportation of ions through cement-based materials: 3. Experimental-evidence for the basic equations and some important deductions, *Cem Concr Res* 24 (1994) 1229–1236.
- [22] O. Truc, J.P. Ollivier, L.O. Nilsson, Numerical simulation of multi-species diffusion, *Mater Struct*, (in press).
- [23] C. Andrade, Calculation of chloride diffusion coefficients in concrete from ionic migration measurements, *Cem Concr Res* 23 (1993) 724–742.
- [24] L. Tang, Concentration dependence of diffusion and migration of chloride ions: Part 2. Experimental evaluations, *Cem Concr Res* 29 (1999) 1469–1474.
- [25] L.N. Plummer, D.L. Parkhurst, G.W. Fleming, S.A. Dunkle, A computer program incorporating Pitzer's equations for calculation of geochemical reactions in brines, *Water Resources Investigations of the USGS*, Reston, USGS, Reston, 1998, pp. 1–4.
- [26] K.S. Pitzer, Activity coefficients in electrolyte solutions, in: R.M. Pytkowicz (Ed.), *Theory: Ion Interaction Approach*, CRC Press, Boca Raton, FL, 1979, pp. 157–208.
- [27] C.K. Larsen, Chloride binding in concrete — effect of surrounding environment and concrete composition, PhD thesis, Structural Engineering, NTNU, Trondheim, 1998.
- [28] E.J. Reardon, Problems and approaches to the prediction of the chemical composition in cement/water systems, *Waste Manage* 12 (1992) 221–239.